



**HAL**  
open science

## On the existence of a scattering pre-peak in the mono-ols and diols

Martina Požar, Aurélien Perera

► **To cite this version:**

Martina Požar, Aurélien Perera. On the existence of a scattering pre-peak in the mono-ols and diols. Chemical Physics Letters, 2017, 10.1016/j.cplett.2017.01.014 . hal-01436259

**HAL Id: hal-01436259**

**<https://hal.sorbonne-universite.fr/hal-01436259>**

Submitted on 16 Jan 2017

**HAL** is a multi-disciplinary open access archive for the deposit and dissemination of scientific research documents, whether they are published or not. The documents may come from teaching and research institutions in France or abroad, or from public or private research centers.

L'archive ouverte pluridisciplinaire **HAL**, est destinée au dépôt et à la diffusion de documents scientifiques de niveau recherche, publiés ou non, émanant des établissements d'enseignement et de recherche français ou étrangers, des laboratoires publics ou privés.

# On the existence of a scattering pre-peak in the mono-ols and diols

Martina Požar<sup>1,2</sup> and Aurélien Perera<sup>1</sup>

<sup>1</sup>Laboratoire de Physique Théorique de la Matière Condensée (UMR CNRS 7600), Université Pierre et Marie Curie, 4 Place Jussieu, F75252, Paris cedex 05, France.

<sup>2</sup>Department of Physics, Faculty of Sciences, University of Split, Ruđera Boškovića 33, 21000, Split, Croatia.

## Abstract

We report a computer simulation study of four 1,n-diols (1,2-ethanediol to 1,5-pentanediol). It is found that increasing the alkyl chain length increases chain-like clusters, and correspondingly the structure factor pre-peak, just like for mono-ols. However, our calculated Xray intensities show that the pre-peak tends to diminish to a shoulder, in contrast with mono-ols where the pre-peak becomes more apparent with increasing alkyl chain. We attribute this contrasting finding to the fact that the alkyl chain is constrained between the two hydroxyl groups in linear diols, while they are free in linear mono-ols.

## 1 Introduction

Associated liquids differ from simple liquids since these latter contain only free particles, while the former contain in addition various “living” clusters of associated particles[1, 2]. Perhaps the simplest way to represent this difference, would be to compute, for both systems, the cluster probability distribution as a function cluster size. Even though such distribution is inherently biased by the various criteria to decide how a given particle belongs to a cluster [3, 4], the two types of distribution differ by the fact that, for simple liquids this distribution is a monotonously decaying function[3, 4], while for associating liquids one expects

1  
2  
3  
4  
5 a peak at some cluster size corresponding to typical representative of associated  
6 particles[5, 6]. Indeed, in a simple liquid, the probability of finding a monomer is  
7 always greater than a dimer, which is larger than for a trimer, and so forth. **There-**  
8 **fore the cluster distribution is a monotonously decaying curve.** Typical examples  
9 are hard sphere or Lennard-Jones liquids for the simple liquids [7]. For associat-  
10 ing liquids, the existence of these living clusters should favour some characteristic  
11 size over isolated monomers, **hence producing a non-monotonic cluster distribu-**  
12 **tion.** Typical examples for such associating liquids are linear alcohols, namely  
13 **mono-ols**[5, 6]. A notable exception is water, for which the cluster distribution  
14 is found to be monotonous [8]. The rationalisation of this behaviour is that wa-  
15 ter has a tetrahedral coordination, which makes the probability of large clusters  
16 always smaller than that of smaller clusters[5, 6, 8]. The situation is entirely dif-  
17 ferent for linear mono-ols, which form chain-like clusters, which decreases the  
18 monomer probability compared to that of some mean labile chain. **Since these as-**  
19 **sociated liquids contain both free monomers and chain-like associated monomers,**  
20 **it is tempting to consider them as a pseudo-mixture of two species:** a mixture  
21 of monomers and labile clusters. This type of consideration has been previously  
22 considered only for water, for which the existence of two types of liquids has been  
23 a paradigm since the early works of Frank [9], and is exacerbated by the experi-  
24 mental evidence of two forms of high and low density amorphous ice (HDA and  
25 LDA) [10], and the recent controversies raised by the search for a putative liquid-  
26 liquid phase separation [11, 12, 13]. **It is quite intriguing that this mixture idea**  
27 **has been used for water, which has a monotonous cluster distribution, but not for**  
28 **linear mono-ols, which do show a singularity in the cluster distribution.**

29  
30  
31  
32  
33  
34  
35  
36 From the experimental side, radiation scattering experiments on alcohols, and  
37 in particular mono-ols, reveal a scattering pre-peak[14, 15, 16, 17, 18, 19]. This  
38 pre-peak is absent from simple liquids such as the Lennard-Jones liquids and  
39 weakly polar liquids[20]. Therefore, the existence of a radiation pre-peak is one  
40 possible signature of particle association. For mono-ols, the pre-peak has been  
41 related to the existence of clusters [21]. Again, such pre-peak is absent for liquid  
42 water [22], signaling the intriguing peculiarity of this liquid[23]. Scattering pre-  
43 peaks have been recently discussed in room temperature ionic liquids, in relation  
44 to the association of charged groups and their segregation from the neutral atomic  
45 groups[24, 25, 26].

46  
47  
48 These two approaches to detect associating liquids can be profitably used for  
49 the case of linear diols. Indeed, in the case of linear mono-ols, the hydroxyl  
50 groups can associate freely in chain patterns, while the oily tails are randomly  
51 distributed. In diols, however, these tails are constrained by the second hydroxyl  
52 group attached at the other end. In such case, the length of the oily tail should play  
53 an interesting role in the association of the end hydroxyl groups. In turn, such a  
54 constraint should influence the clustering properties, and it would be interesting  
55  
56  
57  
58  
59  
60  
61  
62  
63  
64  
65

1  
2  
3  
4  
5 to examine how much these differ from associated liquids such as mono-ols and  
6 water. This study is also interesting in [an attempt](#) to classify various two-liquids.

7  
8 In the present study we examine the structural properties of 1,2-ethanediol  
9 (ethylene glycol) and 1,4-butanediol, in comparison with methanol and ethanol,  
10 respectively, as well as 1,3-propanediol and 1,5-pentanediol, by using molecu-  
11 lar dynamics simulation techniques. Ethylene glycol has been previously studied  
12 through computer simulations by several authors [27, 28, 29, 30]. These studies  
13 confirm that computer simulations of these liquids are robust enough when com-  
14 pared to experiments on real systems. The focus of the present paper differs from  
15 that of the previous studied principally because it is centered around the cluster  
16 and two-liquids structures, in relation to detecting these labile clusters through  
17 cluster and radiation scattering (Xray) analysis, conducted with computer simu-  
18 lation techniques. The main result of our study is that the presence of the oily  
19 chain between the hydroxyl groups hinders their chain association, when com-  
20 pared to the role of the free alkyl chains of mono-ols. In particular, we predict  
21 that the Xray scattering pre-peak of linear diols tends to vanish with increasing  
22 chain lengths, by merging with the main peak. This is in contrast with mono-ols  
23 where this tendency is exactly the opposite: the pre-peak and main peak become  
24 more separated with increasing alcohol chain length[21]. This is even more sur-  
25 prizing, since we equally find evidence of chain-like association of the hydroxyl  
26 groups in both type of systems. The first evidence comes from the probability of  
27 chain-like clusters which increases with chain length, just like for mono-ols. The  
28 second evidence comes from the atomic structure factors of the hydroxyl groups,  
29 which equally show the increase of the pre-peak with alkyl chain length. The rea-  
30 son for this contrasting behaviour comes precisely from the fact that the methyl  
31 groups are *constrained* between the two hydroxyl groups, hence they contribute  
32 very differently to scattering intensities, than the mono-ols.  
33  
34  
35  
36  
37  
38  
39  
40

## 41 **2 Simulation details**

42  
43  
44 As in our previous computer simulation studies, we used the Gromacs program  
45 package [31]. We chose the TraPPE (Transferable Potential for Phase Equilibria)[32]  
46 for diols, while neat mono-ols were modeled with both TraPPE [33] and OPLS  
47 (Optimized Potentials for Liquid Simulations) [34] force fields for the sake of  
48 comparison. Previous works [27, 28, 29, 30] mostly used OPLS or modified  
49 OPLS force fields. In what structural properties of alcohols are concerned, the  
50 differences are minor, as shown below. It should be noted that the all present  
51 simulations allow for flexibility of the alkyl chains. However, this flexibility is  
52 limited, as was previously noted by other authors[27]. [Table I summarises all the](#)  
53 [non-bonded force field parameters.](#) For the diols, we use the notation M1 and M2,  
54  
55  
56  
57  
58  
59  
60  
61  
62  
63  
64  
65

1  
2  
3  
4  
5 respectively, for the methyl/methylene sites closer to the hydroxyl group, and the  
6 next one down the alkyl chain.

7  
8 The initial configurations were generated with Packmol[35] from the appropriate  
9 pdb files. All system sizes were chosen for  $N=1000$  molecules, which was  
10 found to be sufficient to ensure proper asymptotic decay of the various site-site  
11 pair correlation functions. The systems were simulating the ambient condition  
12 liquids, in the isobaric-isothermal (constant  $NpT$ ) ensemble. The temperature  
13 of  $T = 300\text{K}$  and pressure of  $p = 1$  bar were kept constant with the v-rescale  
14 thermostat[36] and Parrinello-Rahman barostat[37].

15  
16 The simulation protocol was the same for all alcohols. After assembling the  
17 initial configurations, the system energy was minimized, followed by equilibra-  
18 tions in the  $NpT$  ensemble for a total of 2 ns. The subsequent production runs  
19 lasted 2 ns and yielded at least 1500 configurations for each alcohol.

20  
21 The clustering of the all the atomic sites, and in particular the hydroxyl groups  
22 were computed. The cluster is defined as the group of particles where each particle  
23 has at least one connection with the neighbor particles. The connectivity criteria  
24 can be geometrical constraints, or for example the Hills energetic criteria where  
25 particles are consider to be connected if their attractive interaction energy is higher  
26 then their relative kinetic energy[38]. In this work, we use the Stillinger distance  
27 criteria [4] where the cutoff distance is defined by the first minima of the site-site  
28 pair distribution function. This way, the bonding between particles are indirectly  
29 related to their interactions as refleted by their pair distribution function. The  
30 cluster size distributions are calculated for the clustering of the like-like sites,  
31 using several different statistical approaches. The cluster size probability function  
32 is evaluated as:

$$33 \quad s_n = \frac{\sum_{k=1}^{N_c} s(n, k)}{\sum_{k=1}^{N_c} \sum_{j=1}^{N_{mol}} s(j, k)}$$

34  
35 where  $s_n$  is the probability for the cluster formed of  $n$  sites,  $s(k, n)$  represents the  
36 number of clusters of the size  $n$  in the configuration  $k$ . Varying the contact distance  
37 between neighbouring atoms that are part of a cluster distance around the first  
38 minima, shows a relative robustness in the resulting cluster distributions[5, 6]. The  
39 cutoff distances defined in this work are  $r_c = 3.7\text{\AA}$  between oxygen atoms,  $r_c =$   
40  $4.5\text{\AA}$  between the M1 and M2 pseudo atoms (see Table I). The cluster distribution  
41 features are quite robust to this choice, except in the case of ethanediol, which we  
42 discuss later below. Cluster size distributions were calculated with the Gromacs  
43 module *g\_clustsize*.

44  
45 The coordination number between atoms  $i$  and  $j$  is defined as:

$$46 \quad n_{ij}(r) = 4\pi \frac{N_i}{V} \int_0^r r^2 g_{ij}(r) dr \quad (1)$$

where  $N_i$  is the number of atoms of types  $i$  in the volume  $V$ .

The atom-atom structure factors are defined in relation to the Fourier transforms of the site-site pair correlation functions  $g_{ij}(r)$

$$S_{ij}(k) = \delta_{ij} + \rho \int d\vec{r} [g_{ij}(r) - 1] \exp(i\vec{k}\cdot\vec{r}) \quad (2)$$

The radiation scattering experiments, in particular Xray scattering experiments such as SAXS and WAXS (small angle and wide angle Xray scattering) measure the scattering intensity, for which we use the Pings-Wasers expression [39], which conveniently allows to express this quantity in terms of the individual structure factors:

$$I(k) = \sum_i f_i(k)^2 + \rho \sum_{i,j} f_i(k) f_j(k) \tilde{h}_{ij}(k) \quad (3)$$

where the sum runs over all type of atoms and the f-functions are the atomic form factors[40].  $\rho = N/V$  is the number of particles  $N$  per volume  $V$ . The  $\tilde{h}_{ij}(k)$  functions are the Fourier transforms of the  $h_{ij}(r) = g_{ij}(r) - 1$ . One can rewrite this expression by using the definition of the structure factor in Eq.(2) as:

$$I(k) = \sum_{ij} f_i(k) f_j(k) S_{ij}(k) \quad (4)$$

The first term in Eq.(3) relates to the ideal contribution to the scattering in the absence of pair correlations (which is also equivalent to  $\rho = 0$ )

$$I_{ideal}(k) = \sum_i f_i(k)^2 \quad (5)$$

We have calculated the Xray scattering intensities using the expressions above. We do not report here the neutron scattering intensities, which differ from the Xray data through the fact that the form factors  $f_i$  are constants (independent of  $k$ ) for neutron scattering, while they have a Gaussian-like shape for Xray scattering. One reason for not reporting this data is because the form factors vary according to whether the various atoms are deuterated or not, which offers too many combinations. The Xray data is independent of such constraints.

Since the force field models used here account for the methyl and methylene groups as a single united atom, it was necessary to find an appropriate form factor for the united atom representation. The procedure chosen here is quite simple: the central carbon-carbon pair correlations and carbon-hydrogen pair correlations are assumed to be the same to the united atom self pair correlations. This amounts to the approximation ( $C$  stands for carbon and  $H$  for hydrogen)

$$h_{CC} = h_{CH} = h_{MM} \quad (6)$$

This is reasonable when there are no charge interactions, and when the sites of the united atom representation are close to each other, which is clearly the case for the carbon and hydrogens atoms associated to methyl and methylene group. If we plug in the approximation Eq.6 into Eq.4, it is quite easy to see that the form factor of the united atom becomes

$$f_M(k) = f_C(k) + n f_H(k) \quad (7)$$

where  $n$  is the number of the hydrogen atoms in the methyl or methylene group.

### 3 Results

We will mostly show comparative results for ethanediol and methanol, and butanediol and ethanol. Results for propanediol and pentanediol are commented whenever necessary. However, we report the calculated intensities for all four diols.

#### 3.1 Snapshots

Fig.1 shows snapshots of the four alcohols. While chain-like patterns of the hydroxyl groups are more apparent in ethanol and butanediol, the case of methanol and ethanediol deserve some comments. From previous studies [41, 42, 43], it is known that methanol has chain-like associations. This is not so apparent in the snapshot as it is for the higher alcohols. The case of ethanediol is more interesting. One sees much less chains, and these tend to be shorter than in methanol. But, one also sees few chains aligned next to each other. This type of alignment overall destroys the single chain detection in the cluster algorithm. Although not shown here, propanediol and pentanediol show chain behaviour similar to butanediol, with a more pronounced chaining for pentanediol.

#### 3.2 Cluster distribution

In order to confirm the visual analysis, we compare in the main panel of Fig.2 the cluster probability distributions of the hydroxyl oxygen atoms, between the four neat liquids. It is seen that, while methanol and ethanol oxygens have a cluster peak about mean cluster size 5, which correspond to that observed in the corresponding snapshots, we note that the cluster structure of butanediol is very similar to that of the mono-ols, however with a smaller monomer probability. This implies that hydroxyl groups are less free in butanediol than in the mono-ols. This is somewhat counter-intuitive, since we expect that the constraint imposed by the alkyl chain would leave fewer hydroxyl groups free. Yet, we observe that there

1  
2  
3  
4  
5 are more bound hydroxyl groups in diols than in the mono-ols. This is equally  
6 the case for propanediol and pentanediol (inset), which both show the cluster  
7 peak corresponding to the observed chaining of the hydroxyl groups. The case  
8 of ethanediol is strikingly different from the others. First, the specific peak is  
9 more of a shoulder than a peak, and second, it looks more like a cluster distribu-  
10 tion of a simple liquid. This can be rationalized in terms of the constraint imposed  
11 by the alkyl chain: the number of free hydroxyl monomers is indeed larger than  
12 for the 3 other alcohols. The cutoff dependence (full versus dashed line) shows  
13 a larger dependence for ethanediol than for the other alcohols (not shown). **The**  
14 **methyl/methylene groups of diols have a monotonously decaying cluster distri-**  
15 **bution, just like for neat mono-ols[5, 6]. This is shown for butandiol in dashed**  
16 **lines in the inset. Since these groups go in pairs in each molecules, the monomer**  
17 **distribution is slightly lower than the dimers. This overall monotonous cluster dis-**  
18 **tribution implies that, despite the constraint of being tied to the clustered hydroxyl**  
19 **groups, these methyl groups are essential randomly distributed.**

### 24 25 26 **3.3 Pair correlation functions**

27  
28 Fig3 shows the pair correlation functions for ethanediol (left panel) and methanol  
29 (right panel). The typical feature of a hydrogen bonded system are observed for  
30 the oxygen and hydrogen pair correlations: a first sharp peak, followed by de-  
31 pleted pair correlations of the nearest next neighbours. This depletion is due to  
32 the underlying charge ordering [44]. Indeed, hydrogen bond association is mod-  
33 eled by Coulomb interactions, and these impose the alternate distribution of plus  
34 and minus charges, which is called charge ordering[45, 46]. In a system con-  
35 strained by the presence of neutral groups, charge ordering often takes the shape  
36 of chain-like pattern of the plus and minus charges, thus depleting their isotropic  
37 distribution. These typical features of increased first pair correlations, accom-  
38 panied by a depressed pair correlation produces the pre-peak in the associated  
39 structure factor [44]. The carbon group pair correlations are very much LJ-like,  
40 as expected. The main difference between the ethanediol and methanol is in the  
41 height of the first peaks, and perhaps a more marked depletion of second neigh-  
42 bours. This is expected on the basis of the constrained versus free alkyl chains  
43 argument. For methanol, we have shown a comparison with the OPLS force field  
44 (in dashed lines) and it is clearly seen that the difference between the TraPPE and  
45 OPLS force fields is negligible, at least in what concerns structural properties.

46  
47 Fig4 shows the pair correlation for butanediol(left) and ethanol(right). Fea-  
48 tures similar to those described above are seen again, as expected because of the  
49 similarities of these systems. We observe that the hydrogen bonding first peaks  
50 are higher than in the respective previous cases, while the depletion is not so much  
51 more marked. This is in support of the increased chaining pattern, and in align-  
52  
53  
54  
55  
56  
57  
58  
59  
60  
61  
62  
63  
64  
65

1  
2  
3  
4  
5  
6  
7  
8  
9  
10  
11  
12  
13  
14  
15  
16  
17  
18  
19  
20  
21  
22  
23  
24  
25  
26  
27  
28  
29  
30  
31  
32  
33  
34  
35  
36  
37  
38  
39  
40  
41  
42  
43  
44  
45  
46  
47  
48  
49  
50  
51  
52  
53  
54  
55  
56  
57  
58  
59  
60  
61  
62  
63  
64  
65

ment with the observations of the previous sections. We note again that hydrogen bonding in butanediol is smaller than in ethanol. We equally note that the pair correlations between the methyl sites are in phase for ethanol, but dephased for butanediol. This is an important indication, which will serve us to explain the radiation scattering data below.

Fig.5 shows the coordination number of the oxygen sites, which complements the information found in the snapshot and cluster distributions. It is found that the first peak and minimum of  $g_{OO}(r)$  contributes to a marked inflexion of the coordination around 2 neighbours in average. This is fully consistent with the existence of linear clusters of the hydroxyl sites. This is less apparent for ethanediol, again in good agreement with the lesser presence of such clusters in this system.

The structural features for propanediol and pentanediol are very similar to butanediol, and are not reported here.

### 3.4 Structure factors

Fig.6 shows the various atom-atom structure factors of the pair correlations displayed in Fig.3. The presence of the pre-peak at  $k_P \approx 1 \text{ \AA}^{-1}$  is clearly noticeable. The main peak is given by the methyl site pair correlation at  $k_M \approx 2\pi/\sigma_M$ , and depends on the methyl site diameter  $\sigma_M \approx 3.5$ . The pre-peak is more marked for the methanol than for the ethanediol pair correlations. This is consistent with the fact that the cluster structure of the latter system is less pronounced than that of the former. We equally note that the double peak structure of the pre-peak “plateau” like feature in  $S_{OO}(k)$  is in fact due to the dual contributions of the OH peak at  $k_P \approx 1 \text{ \AA}^{-1}$  and the main peak at  $k_M \approx 2\pi/\sigma_M$ . It is interesting to note that the pre-peak at  $k_P \approx 1 \text{ \AA}^{-1}$  is equally found in the recently reported total structure factor in neutron scattering experiments[47], and the whole shape is very similar to that we report here.

Fig.7 shows the structure factors for the butanediol and ethanol corresponding to the pair correlation shown in Fig.4. The pre-peak is much more pronounced than in the previous case, witnessing better cluster structures and confirming general trends deduced from previous analysis. We equally observe that the pair correlations between the methyl sites are out of phase for butanediol and in phase for ethanol.

The pre-peak feature for propanediol and pentanediol are quite similar to those reported above, with an increased pre-peak and decreasing main peak trend with increasing alkyl chain length. This is in line with the cluster plot (inset of Fig.2) and the visually observable chains in the snapshots for both these systems. Some of these structure factors are reported below in Fig.8.

### 3.5 Scattering intensity

The Pings-Wasers Xray scattering intensity is calculated from the expression given in Eq.(3), with the atom-atom structure factors calculated and shown in the previous sub-section. Fig.8 shows the SAXS data for all four diols, together with those calculated for the mono-ols, and experimental SAXS data from Ref.[21] for ethanol. In each panels, the main intensity  $I(k)$  is reported in blue lines, and the ideal intensity  $I_{ideal}(k)$  (Eq.5) in green lines (dashed lines for the mono-ols). It is seen that, despite the fact that the pre-peak structure of butanediol is better defined from that of ethanediol, the scattering intensity shows a less pronounced contribution for the former. This trend becomes more apparent for propanediol and pentanediol, for which only the main peak is apparent, and the pre-peak is just a shoulder. This is in variance with linear mono-ols, for which the pre-peak is more pronounced for longer chains[21]. We relate this finding with the fact that the carbon site contributions are i) more numerous for longer diols and ii) out of phase for the longer diols and distributed between  $k_P$  and  $k_M$ . This contributes to enhance the contributions at  $k_M$ , while smearing that at  $k_P$ . This important finding remains to be confirmed experimentally as well.

It is interesting to note that the individual  $S_{ij}(k)$  are not primary experimental observables, unlike  $I(k)$ . However, there exist procedures to rebuild the  $S_{ij}(k)$  by isotope weighting techniques of the various atomic contributions. This holds only for neutron scattering data. In the case of Xray scattering, this usual procedure is to rebuild  $I(k)$  from the computed  $S_{ij}(k)$ . If the pre-feature is almost erased from the final  $I(k)$ , one wonders which procedure would restore it in the individual  $S_{ij}(k)$ . It seems more likely that these contributions are likely to remain smeared, leading to discrepancies in the comparison between the simulated and re-computed  $S_{ij}(k)$ , which would be totally artificial.

## 4 Discussion and Conclusion

If the hydroxyl endgroup of any alcohol molecule is identified to a dipolar or magnetic “charge”, then linear mono-ols are free “charges”, while linear diols are constrained “charge” pairs, constrained by the intermediate alkyl chain. This analogy with magnetic systems, in particular with monopoles, which has attracted a recent renewed interest[48, 49], hints to the importance the constraint between the two hydroxyl groups can have. In this “molecular representation” of the magnetic problem, it is how the local order evolves with the constraint length, which becomes the appealing comparison factor. In this context, the association of these charges into chains bears a different meaning, according to the case when the charges are free or tied by the alkyl chains. What the present study shows

1  
2  
3  
4  
5 is that, independently of the alkyl-chain tying constraints, increasing the chain  
6 length leads to better chain-like association of the hydroxyl “charges” both in  
7 mono-ols and diols. However, the presence of the constraint influences markedly  
8 the scattering function, by smearing the pre-peak and the main peak into a single  
9 feature. This means that experimental detection of the chain pre-peak in diols is  
10 rendered difficult or even impossible through radiation scattering experiments, as  
11 opposed to mono-ols. This means that, in the absence of an independent statistical  
12 description, such as computer simulations for example, it would be difficult to tell  
13 if specific forms of clusters can appear in some types of associating liquids, such  
14 as diols. This “invisibility” of a microscopic feature through a given experiment  
15 is an intriguing aspect of the present work.

16  
17  
18  
19 This problem of the invisibility of a microscopic feature through radiation  
20 scattering experiments was equally met in our previous studies of aqueous mix-  
21 tures of mono-ols (as well as other polar solutes), where strong pre-peak are  
22 observed in atom-atom structure factors obtained from simulations, while there  
23 seems to be no evidence of them in Xray or neutron scattering data[50]. The  
24 present system then provides one solution to this seemingly generic enigmatic  
25 finding between scattering and computer experiments, which concerns the prob-  
26 lem of a direct experimental detection of the microscopic heterogeneity.  
27  
28  
29

## 30 31 **Acknowledgments**

32  
33  
34 This work has been supported in parts by the Croatian Science Foundation for fi-  
35 nancial support under the project 4514 “Multi-scale description of meso-scale do-  
36 main formation and destruction”. M. Požar thanks the French Embassy in Croatia  
37 for financial support through “bourse du Gouvernement Français”.  
38  
39  
40

## 41 **References**

- 42  
43  
44 [1] A. Stradner, H. Sedgwick, F. Cardinaux, W. C. K. Poon, S. U. Egelhaaf and  
45 P. Schurtenberger, *Nature* **432**, 492 (2004)  
46  
47 [2] A. J. Archer, N. B. Wilding, *Phys. Rev.* **E 76**, 031501 (2007)  
48  
49 [3] L. A. Pugnaloni and F. Vericat, *J. Chem. Phys.*, 116, 1097 (2002).  
50  
51 [4] F. H. Stillinger, *J. Chem. Phys.*, 38, 1486 (1963).  
52  
53 [5] A. Perera, F. Sokolic and L. Zoranic, *Phys. Rev.*, E75, 060502-(R) (2007).  
54  
55 [6] L. Zoranic, F. Sokolic and A. Perera, *J. Chem. Phys.*, 127, 024502 (2007).  
56  
57  
58

- 1  
2  
3  
4  
5 [7] H. Jonsson and H. C. Andersen, Phys. Rev. Lett., 60, 2295 (1988).  
6  
7 [8] A. Geiger, F. H. Stillinger and A. Rahman, J. Chem. Phys., 70, 4185 (1979).  
8  
9 [9] H.S. Frank and A.S. Quist, J. Chem. Phys. 34, 604 (1961)  
10  
11 [10] O. Mishima, L. D. Calvert and E. Whalley, Nature 314, 76-78 (1985)  
12  
13 [11] O. Mishima and H.E. Stanley, Nature 392, 164-168 (1998).  
14  
15 [12] P.H. Poole, F. Sciortino, U. Essmann, H. Stanley, Nature 360, 324-328  
16 (1992).  
17  
18 [13] P. Gallo, K. Amann-Winkel, C. A. Angell, M. A. Anisimov, F. Caupin, C.  
19 Chakravarty, E. Lascaris, T. Loerting, A. Z. Panagiotopoulos, J. Russo, J. A.  
20 Sellberg, H. E. Stanley, H. Tanaka, C. Vega, L. Xu, and L. G. M. Pettersson,  
21 Chemical Reviews 116, 7463-7500 (2016).  
22  
23 [14] B. E. Warren, Phys. Rev. **44**, 969 (1933).  
24  
25 [15] A. H. Narten and A. Habenschuss, J. Chem. Phys. **80**, 3387 (1984)  
26  
27 [16] A. H. Narten and S. I. Sandler, J. Chem. Phys. **71**, 2069 (1979)  
28  
29 [17] D. G. Montague, J. C. Dore and S. Cummings, Mol. Phys. **53**, 1049 (1984)  
30  
31 [18] S. Sarkar and R. N. Joarder, J. Chem. Phys. 99, 2032 (1993)  
32  
33 [19] R. Böhmer, C. Gainaru and R. Richert, Phys. Rep. **545**, 125 (2014)  
34  
35 [20] J.P. Hansen and I.R. McDonald, *Theory of Simple Liquids* (Academic, Lon-  
36 don, 1986)  
37  
38 [21] M. Tomšič, A. Jamnik, G. Fritz-Popovski, O. Glatter and L. Vlcek, J.  
39 Phys.Chem. **B 111**, 1738 (2007)  
40  
41 [22] T. Head-Gordon and H. Hura, Chem. Rev. **102**, 2651 (2002)  
42  
43 [23] A. Perera, Mol. Phys. **109**, 2433 (2011)  
44  
45 [24] A. Triolo, O. Russina, H-J Bleif and E. Di Cola, J. Phys. Chem. **B111**, 4641  
46 (2007)  
47  
48 [25] H. V. R. Annapureddy, H. K. Kashyap, P. M. De Biase and C. J. Margulis, J.  
49 Phys. Chem. **B114**, 16838 (2010)  
50  
51 [26] Y. Wang, W. Jian, T. Yan and G. A. Voth, Acc. Chem. Res. **40**, 1193 (2007)  
52  
53  
54  
55  
56  
57  
58  
59  
60  
61  
62  
63  
64  
65

- 1  
2  
3  
4  
5 [27] L. Saiz, J. A. Padró, and E. Guàrdia, *The Journal of Chemical Physics* **114**,  
6 3187 (2001)  
7  
8 [28] A. V. Gubskaya and P. G. Kusalik, *J. Phys. Chem. A* **108**, 7151-7164 (2004)  
9  
10 [29] O. Vital de Oliveira and L.C. Gomide Freitas, *Journal of Molecular Struc-*  
11 *ture: THEOCHEM* **728**, 179 (2005)  
12  
13 [30] A. Kaiser, O. Ismailova, A. Koskela, S.E. Huber, M. Ritter, B. Cosenza, W.  
14 Benger, R. Nazmutdinov, M. Probst, *Journal of Molecular Liquids* **189**, 20  
15 (2014)  
16  
17 [31] D. van der Spoel, E. Lindahl, B. Hess, G. Groenhof, A. E. Mark and H.J.C.  
18 Berendsen, *J.Comp. Chem.* **26**, 1701 (2005)  
19  
20 [32] J.M. Stubbs, J.J. Potoff and J.I. Siepmann, *J. Phys. Chem. B* **108**, 17596-  
21 17605 (2004)  
22  
23 [33] B. Chen, J.J. Potoff and J.I. Siepmann, *J. Phys. Chem. B* **105**, 3093-3104  
24 (2001)  
25  
26 [34] W. L. Jorgensen, J. Tirado-Rives, *J. Am. Chem. Soc.* **110**, 1657 (1988)  
27  
28 [35] J. M. Martínez and L. Martínez, *Journal of Computational Chemistry*,  
29 **24**(7):819-825, 2003; *ibid* L. Martínez, R. Andrade, E. G. Birgin, J. M.  
30 Martínez. *Journal of Computational Chemistry* **30**, 2157 (2009)  
31  
32 [36] G. Bussi, D. Donadio and M. Parrinello, *J. Chem. Phys.* **126**, 014101 (2007)  
33  
34 [37] M. Parrinello and A. Rahman, *J. Appl. Phys.* **52**, 7182 (1981)  
35  
36 [38] Pugnali L. A. and Vericat F.(2002) *J. Chem. Phys.* **116** 1097 (2002)  
37  
38 [39] J. C. Pings and J. Waser, *J. Chem. Phys.* **48**, 3016 (1968)  
39  
40 [40] *International Tables for Crystallography*, ed. E. Prince, International Union  
41 of Crystallography, 2006, vol. C.  
42  
43 [41] Y. Tanaka, N. Ohtomo, K. Arakawa, *Bull. Chem. Soc. Jpn.* **58** 270 (1985).  
44  
45 [42] T. Yamaguchi, K. Hidaka, A.K. Soper, *Mol. Phys.* **96** 1159 (1999).  
46  
47 [43] J.-H. Guo, Y. Luo, A. Augustsson, S. Kashtanov, J.-E. Rubens- son, D. K.  
48 Shuh, H. Ågren, and J. Nordgren, *Phys. Rev. Lett.* **91**, 157401 (2003)  
49  
50 [44] A. Perera and R. Mazighi, *J. Chem. Phys.*, **143**, 154502 (2015).  
51  
52  
53  
54  
55  
56  
57  
58  
59  
60  
61  
62  
63  
64  
65

- 1  
2  
3  
4  
5 [45] F. G. Edwards, J. E. Enderby and D. I. J. Page, Phys. C: Solid State Phys. **8**  
6 , 3483 (1975)  
7  
8 [46] A. Perera, Phys. Chem. Chem. Phys. DOI: 10.1039/c6cp07834f (2017)  
9  
10 [47] H. Abdelmoulaoui, H. Ghalla, S. Nasr, M. Bahri and M.-C. Bellissent-Funel,  
11 J. Mol. Liq. **220**, 527 (2016)  
12  
13 [48] S. Ladak, D. E. Read, G. K. Perkins, L. F. Cohen and W.R. Branford, Nature  
14 Physics **6**, 359 (2010)  
15  
16 [49] E. Mengotti, L. J. Heyderman, A. F. Rodríguez, F. Nolting, R. V. Hügli and  
17 H.-B. Braun, Nature Physics **7**, 68 (2011)  
18  
19 [50] A. Perera, Pure Appl. Chem. **88**, 189 (2016) .  
20  
21  
22  
23  
24  
25  
26  
27  
28  
29  
30  
31  
32  
33  
34  
35  
36  
37  
38  
39  
40  
41  
42  
43  
44  
45  
46  
47  
48  
49  
50  
51  
52  
53  
54  
55  
56  
57  
58  
59  
60  
61  
62  
63  
64  
65

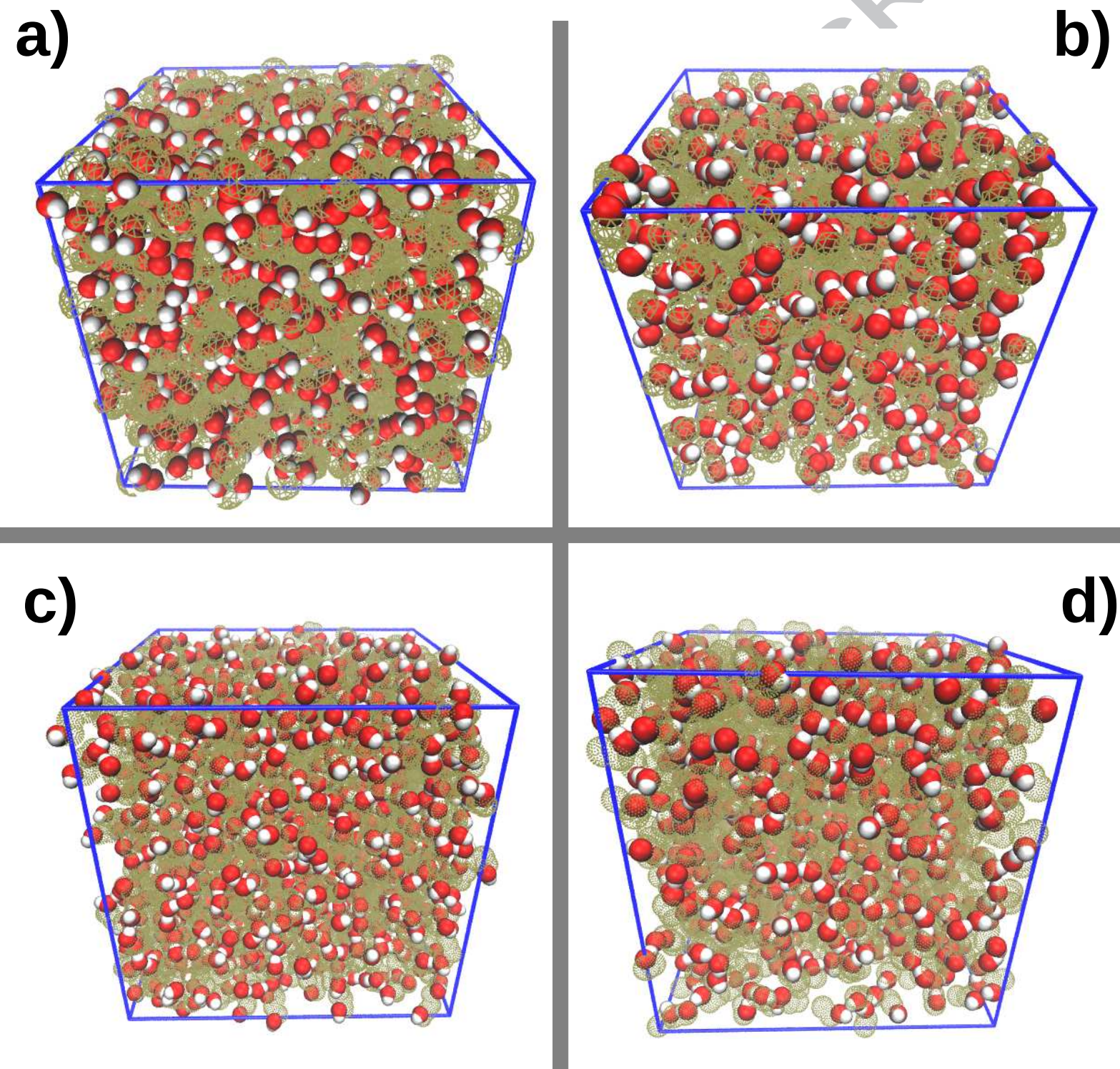
## Table caption

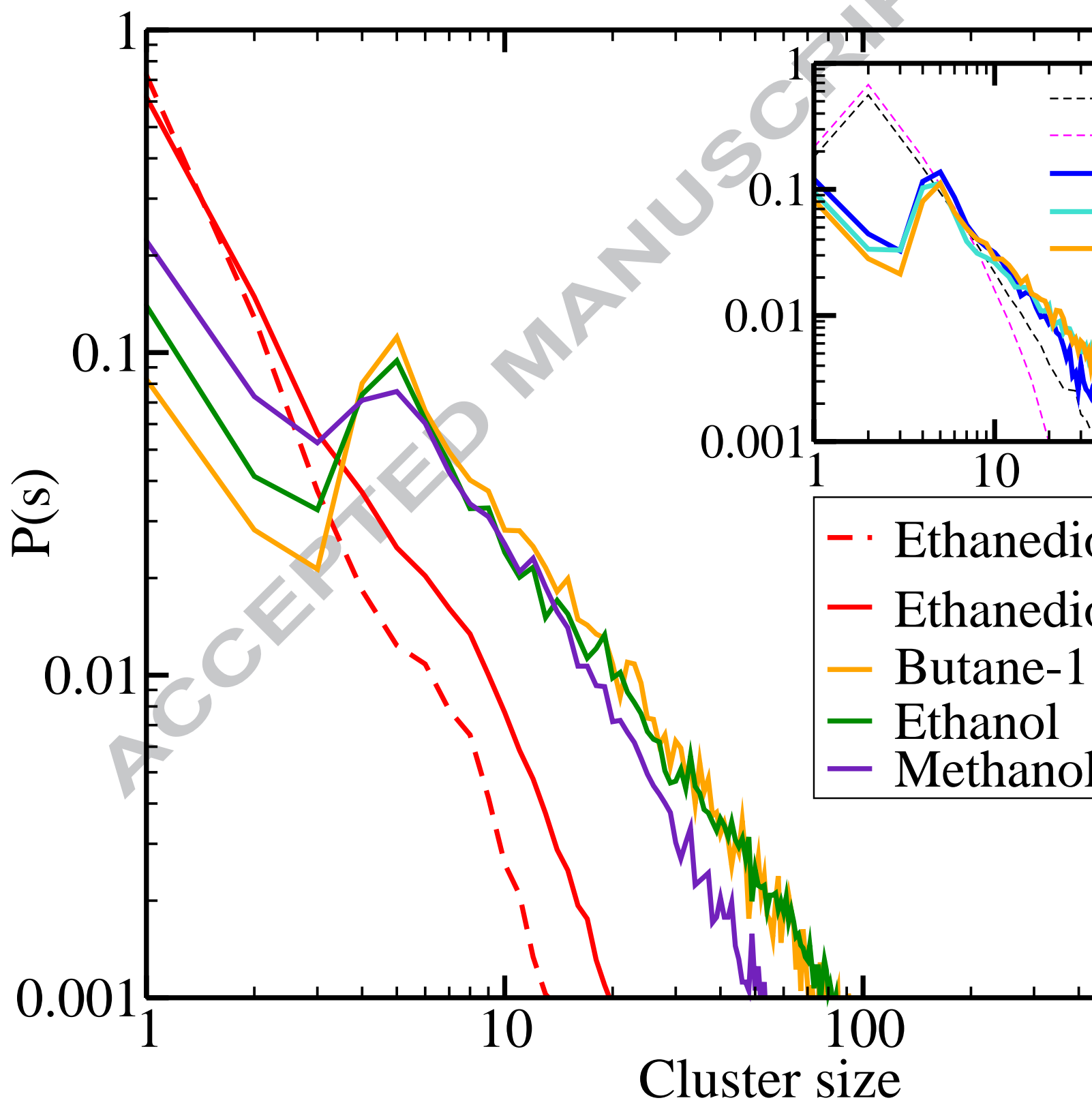
Table 1 - TraPPE and OPLS (only for methanol -data in parenthesis) force field parameters (non-bonded) for diols and mono-ols.

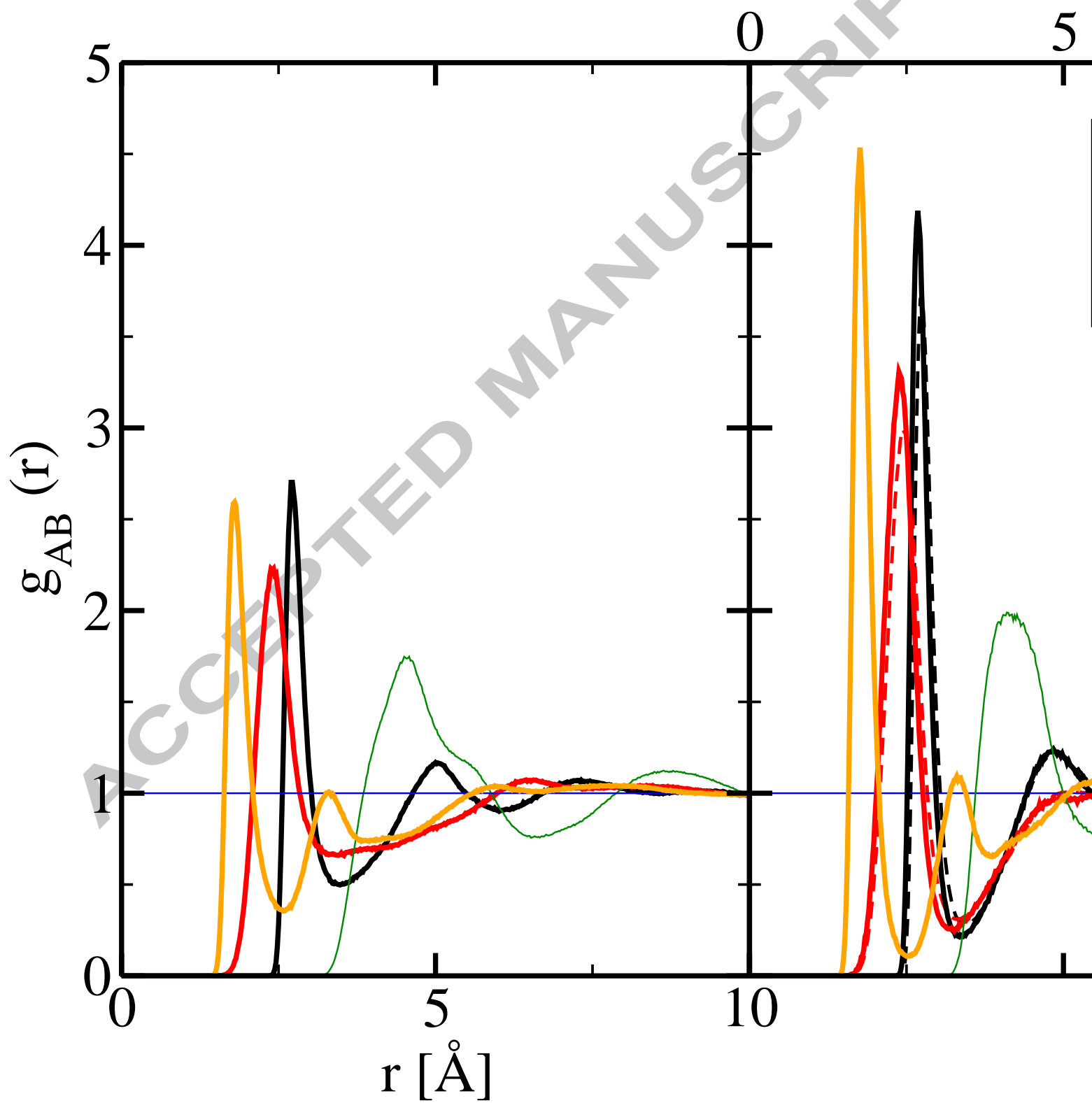
Alcohol	Site	$\epsilon/k_B[\text{K}]$	$\sigma[\text{\AA}]$	$q[e]$
Methanol	$\text{CH}_3(\text{M2})$	98.0 (104.2)	3.750 (3.775)	0.265 (0.265)
	$O$	93.0 (85.6)	3.020 (3.070)	-0.700 (-0.700)
	$H$	0.0 (0.0)	0.000 (0.000)	0.435 (0.435)
Ethanol	$\text{CH}_3(\text{M2})$	98.0	3.750	0.000
	$\text{CH}_2(\text{M1})$	46.0	3.950	0.265
	$O$	93.0	3.020	-0.700
	$H$	0.0	0.000	0.435
1,2-ethanediol	$\text{CH}_2(\text{M2})$	46.0	3.950	0.265
	$O$	93.0	3.020	-0.700
	$H$	0.0	0.000	0.435
1,4-butanediol	$\text{CH}_3(\text{M2})$	46.0	3.950	0.000
	$\text{CH}_2(\text{M1})$	46.0	3.950	0.265
	$O$	93.0	3.020	-0.700
	$H$	0.0	0.000	0.435

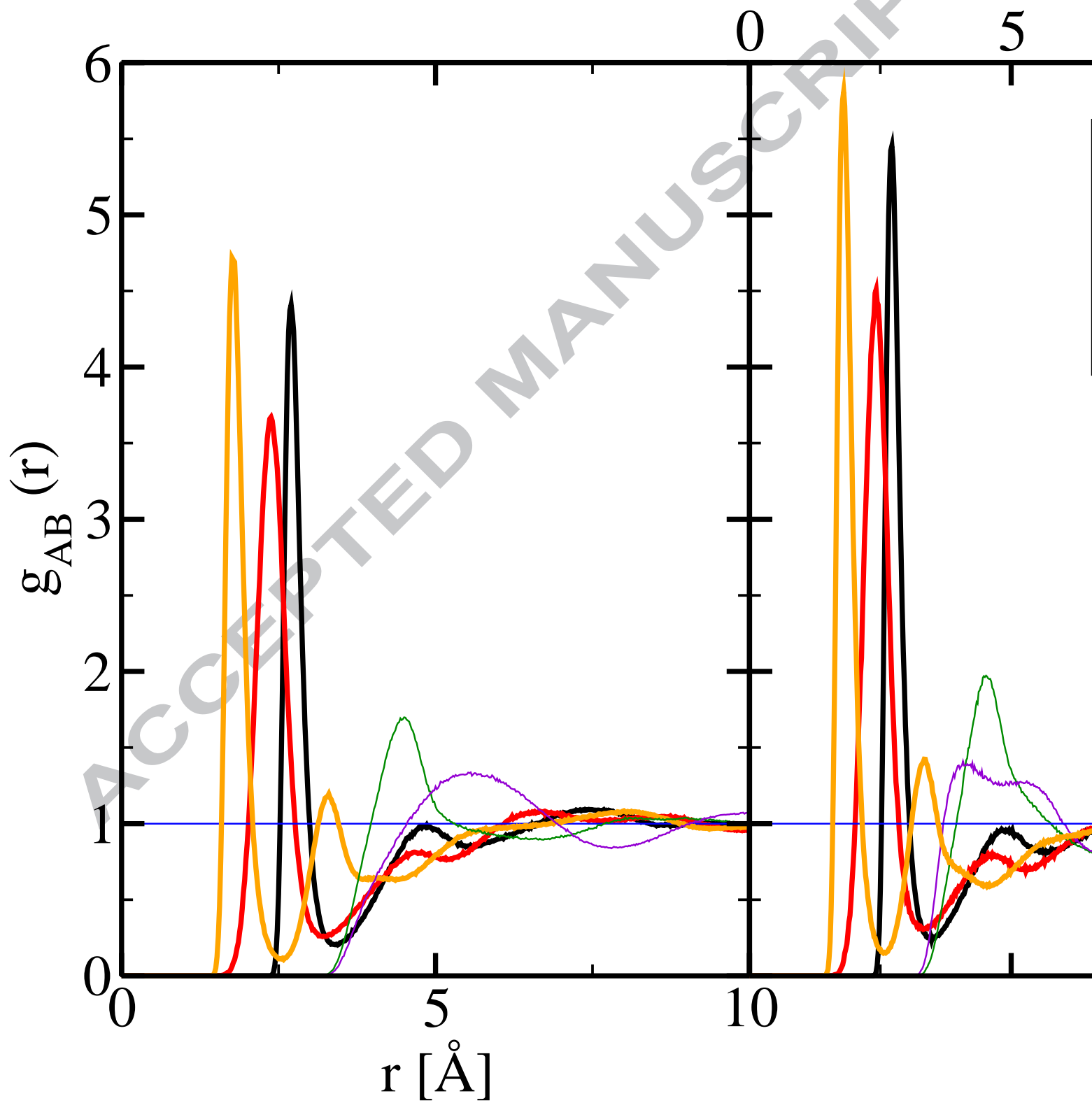
## Figure captions

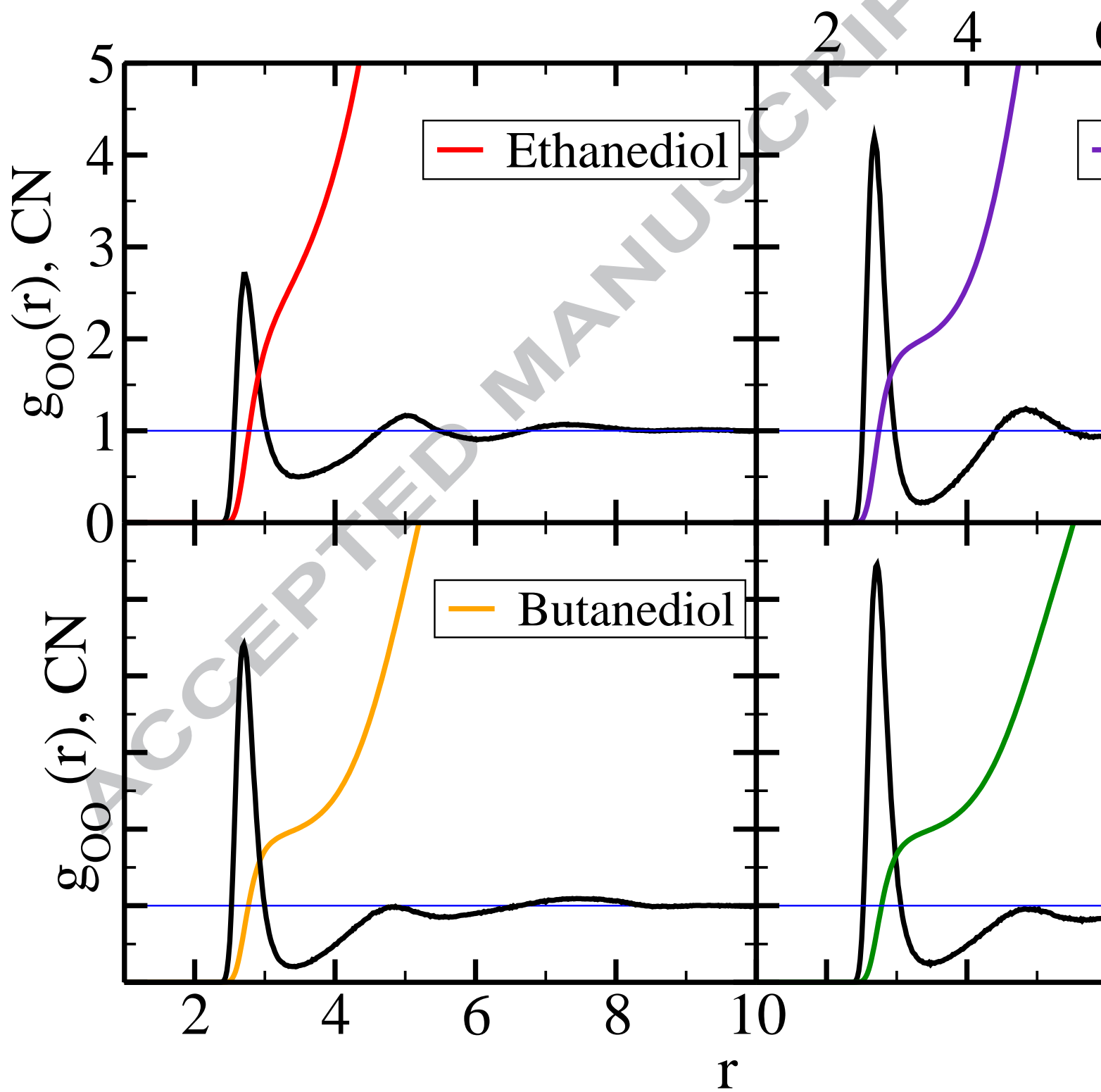
- Fig.1 - Snapshots: (a) ethanediol, (b) methanol, (c) butanediol, (d) ethanol. Oxygen atom is shown in red, hydrogen in white and methyl and methylene united atoms as semi-transparent tan.
- Fig.2 - Cluster probability  $P(s)$  versus cluster size  $s$ . The cutoff parameter is taken to be  $r = 3.6 \text{ \AA}$ , except for ethanediol for which  $r = 3 \text{ \AA}$  and  $r = 2.9 \text{ \AA}$  are reported in dashed and full red lines. Main panel shows a comparison between mono-ols and diols. The inset shows more diols distributions (full lines) and distribution of the methylene sites (M1 and M2) for butanediol.
- Fig.3 - Site-site pair correlation functions for ethanediol (left panel) and methanol (right panel).
- Fig.4 - Site-site pair correlation functions for butanediol (left panel) and ethanol (right panel)
- Fig.5 - Oxygen-oxygen coordination numbers. The  $g_{OO}(r)$  function as shown in black.
- Fig.6 - Site-site structure factors corresponding to the pair correlations shown in Fig.3 for ethanediol (left panel) and methanol (right panel).
- Fig.7 - Site-site structure factors corresponding to the pair correlations shown in Fig.3 for butanediol (left panel) and ethanol (right panel)
- Fig.8 - Calculated Xray scattering intensity  $I(k)$  for diols (in blue). The green curve is the ideal contribution (see text). The scattering curves for mono-ols (methanol and ethanol) are shown in dashed lines under those of ethanediol and butanediol. The experimental Xray data for ethanol[21] is shown in black line. The insets show typical atom-atom structure factors (see text) with a scaled  $I(k)$  (in thick black line), with vertical lines indicating the position of the pre-peak and main peak.

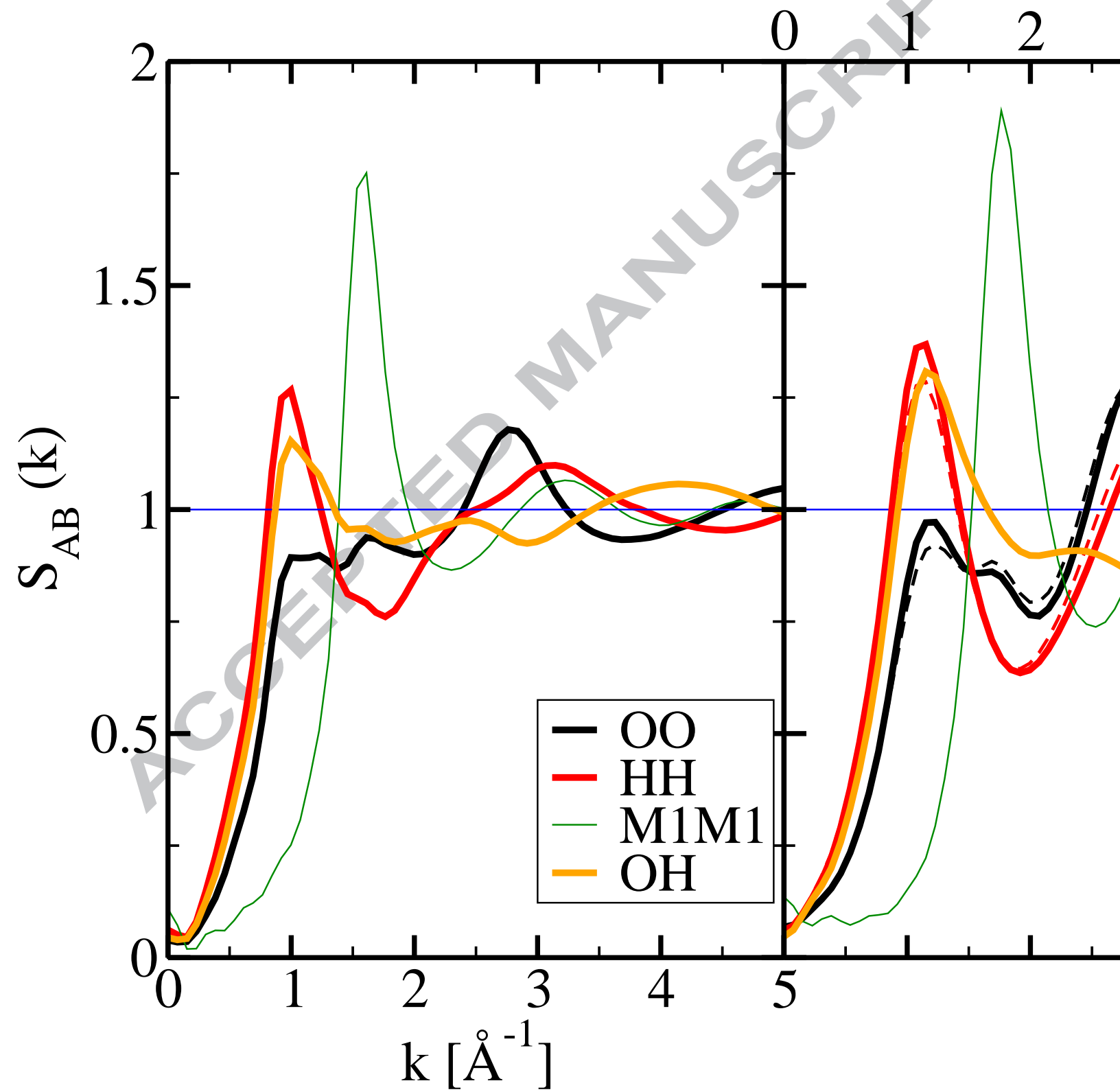


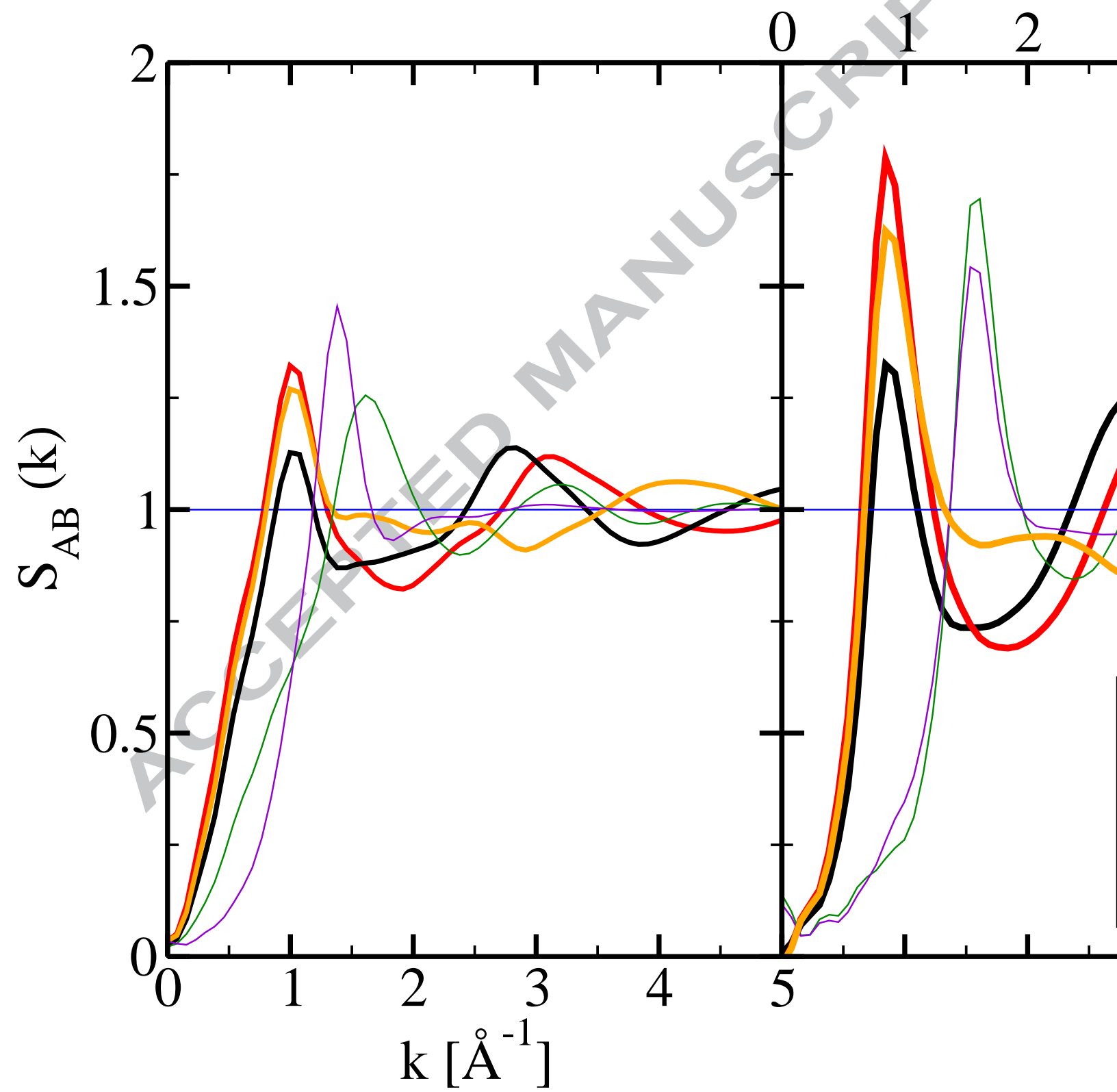




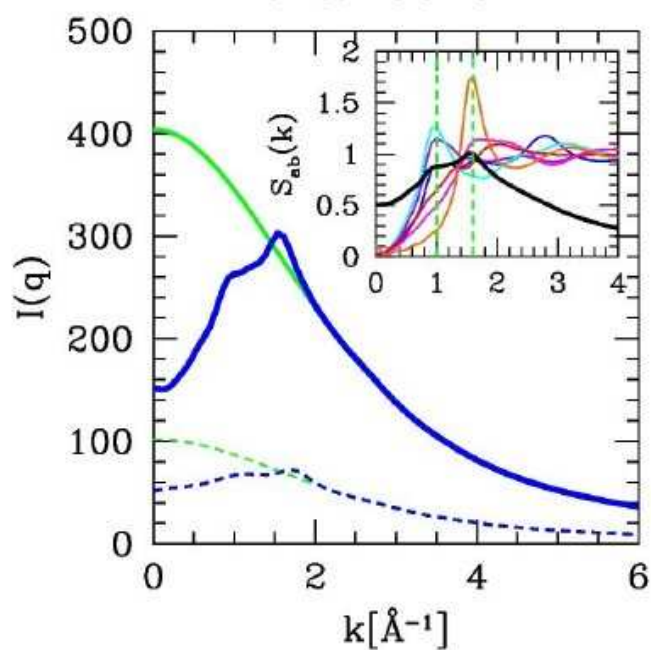
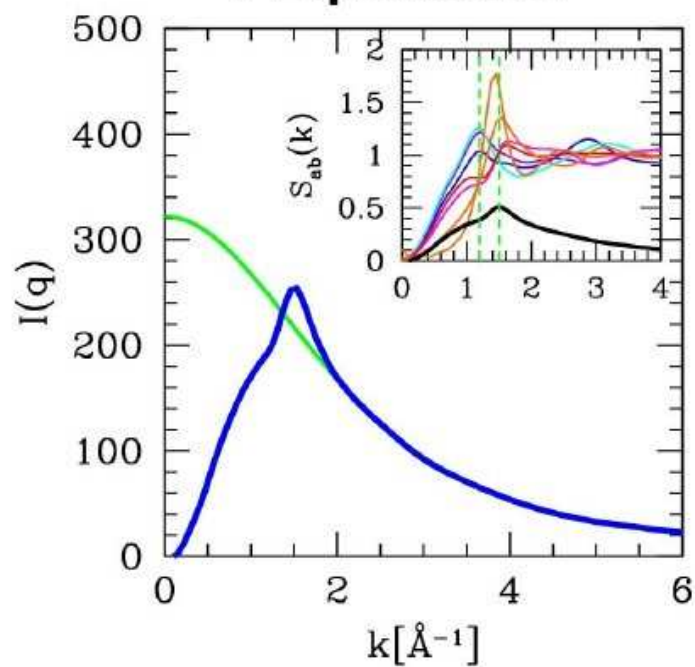
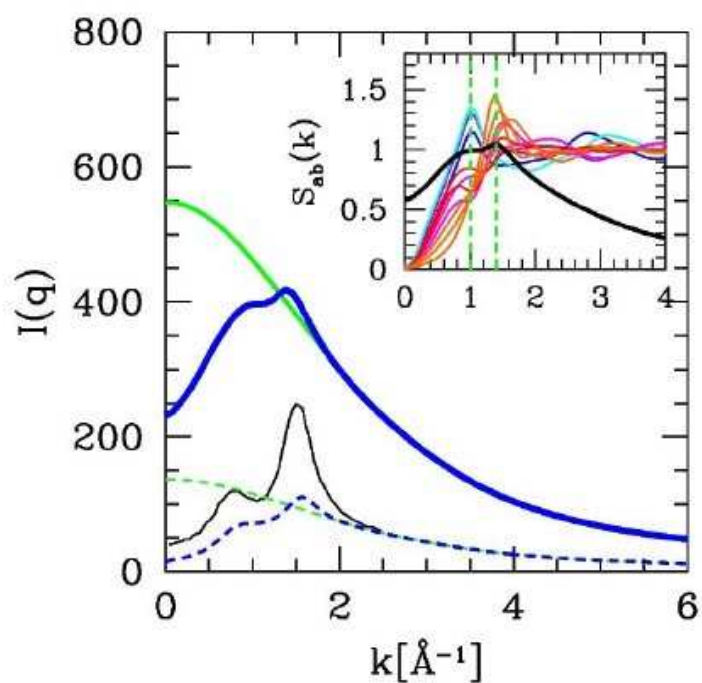
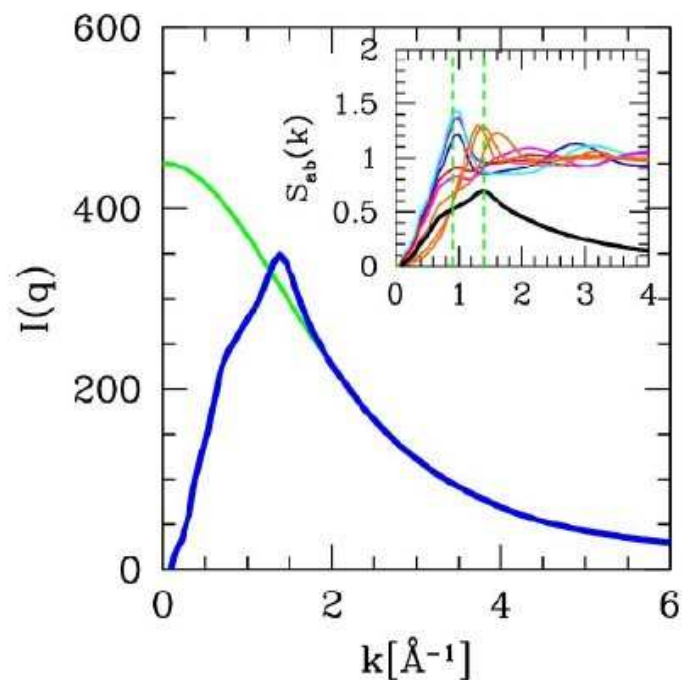


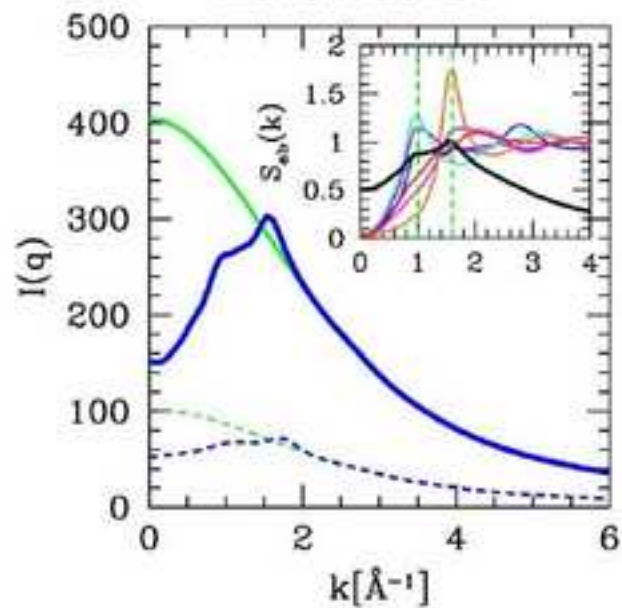
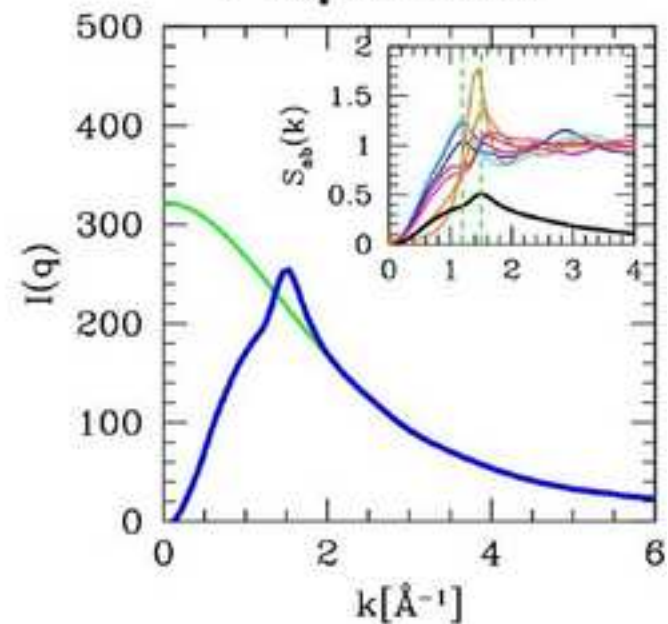
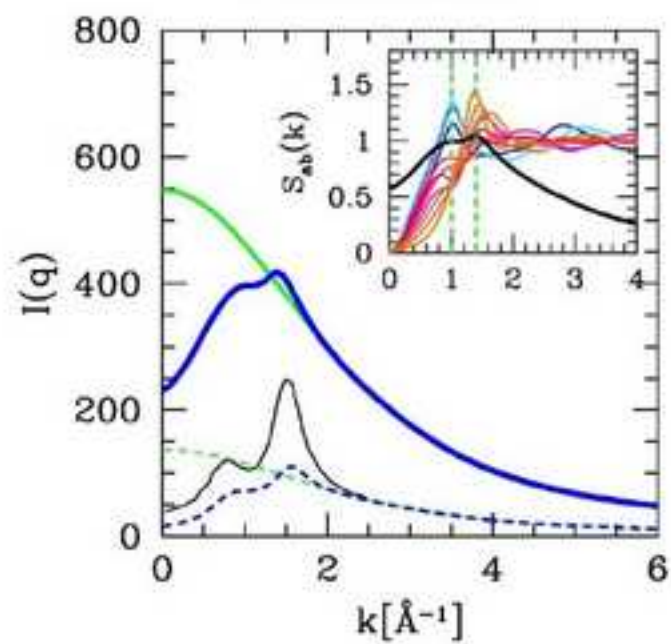
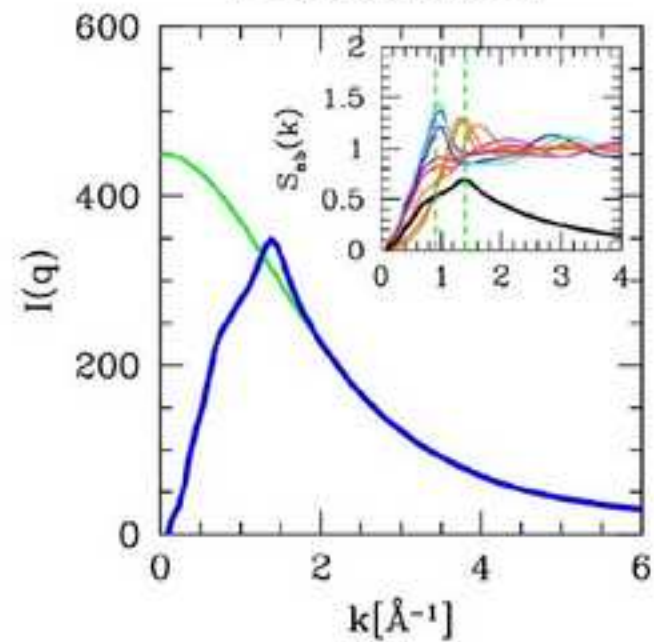






RIPT

**Ethenediol****Propanediol****Butanediol****Pentanediol**

**Ethanediol****Propanediol****Butanediol****Pentanediol**

This work is about comparing the nature of self-aggregation in diols and mono-ols, both through the statistical approach (clusters, correlation functions and structure factors) and calculated X-ray scattering. We find a surprising result, that the similarity in clustering between diols and mono-ols is not replicated by the similarity in the X-ray scattering. The pre-peak feature known in mono-ols seems to disappear in diols. We associate this feature to the fact that hydroxyl groups of the diols are constrained by the alkyl chains. To our knowledge, this is the first report of such difference between mono-ols and diols.

ACCEPTED MANUSCRIPT